MULTI-SCALE STUDY OF REINFORCEMENT VARIABILITY AND VOID FORMATION IN LIQUID COMPOSITE MOULDING

A. Endruweit, F. Gommer, A.C. Long

Faculty of Engineering – Division of Materials, Mechanics & Structures, University of Nottingham, University Park, Nottingham, NG7 2RD, U.K.
andreas.endruweit@nottingham.ac.uk

Keywords: Fabrics/textiles, resin flow, computational simulation, probabilistic methods

Abstract
In the manufacture of composite components employing Liquid Composite Moulding (LCM) processes, resin flow during impregnation of the reinforcement is affected by the stochastic arrangements of yarns in fabrics and of filaments in yarns. The influence of non-uniform distributions of yarns on impregnating resin flow was quantified experimentally in terms of global permeability values and their variability. Local fluid concentrations in partially impregnated reinforcements were mapped, and dry spot development during impregnation was tracked. Geometrical models were developed for yarn distributions in fabrics and chopped random preforms, allowing realistic mould filling patterns to be simulated and the variability in global permeability to be estimated. Yarn permeabilities, which differ significantly from ideal values, were derived from models of non-uniform filament distributions. Probabilities for dry spot formation were assessed.

1 Introduction

In the manufacture of composite components employing Liquid Composite Moulding (LCM) processes, resin flow during impregnation of the fibrous reinforcement is determined by the reinforcement structure. Non-uniformity of the fibrous structure results in different flow velocity of the injected resin in different zones of the reinforcement, which is related to uneven flow front propagation. This results in high variability of mould filling patterns and injection times, which may affect product quality and process cycle times. Of particular concern is the formation of resin-free dry spots and a reduction in the matrix-dominated mechanical properties of the finished component. This study aims at experimental characterisation and numerical modelling of non-uniform reinforcement structures, resin flow patterns and void formation at different scales.

2 Experimental observations

Visual monitoring of radial injection experiments for different reinforcement fabrics indicates that the shapes of propagating flow fronts are related to the fabric architectures. For fabrics from densely packed fine yarns, almost perfectly elliptical flow fronts develop, while flow front shapes differ significantly from an ideal ellipse for coarse fabrics made from thick yarns at relatively wide spacing (Fig. 1). Uneven flow front propagation is related to local non-uniformity of the fabric porosity. Fabric non-uniformity can be expressed in terms of

distributions of fibre angles and fibre spacing, effectively indicating the degree of in-plane yarn waviness, and is related to yarn mobility, which depends on the fabric architecture and tends to increase with (average) yarn spacing. Ultimately, non-uniform flow velocity fields can result in formation of dry spots during fabric impregnation.

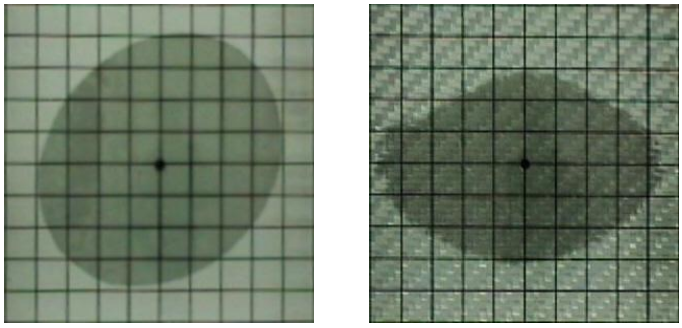

Figure 1. Qualitative comparison of typical flow front shapes in radial injection for examples of woven glass fibre fabrics of different architecture; left: fine fabric structure; right: coarse fabric [1].

Uneven flow front propagation is reflected in the variability in global principal permeabilities, K_1 and K_2, measured in unsaturated radial injection experiments (Table 1). The data in the table suggest that there is a trend for coarse fabrics (with generally high superficial density, S_0) to show high variability in global permeability, while the variability tends to be lower for fine fabrics (low superficial density).

fabric	S_0 / g/m^2	V_f	θ	K_1 /10^{-10} m^2	K_2 / 10^{-10} m^2
± 45° non-crimp, glass fibre	965 ± 4 (± 0.4 %)	0.56 ± 0.00 (± 0.8 %)	112° ± 43°	0.219 ± 0.049 (± 22.5 %)	0.184 ± 0.048 (± 26.1 %)
5-hs satin weave, carbon fibre	393 ± 2 (± 0.4 %)	0.56 ± 0.00 (± 0.0 %)	11° ± 9°	0.328 ± 0.059 (± 17.9 %)	0.246 ± 0.029 (± 12.0 %)
5-hs satin weave, carbon fibre	302 ± 1 (± 0.4 %)	0.61 ± 0.00 (± 0.8 %)	91° ± 1°	0.472 ± 0.047 (± 10.0 %)	0.208 ± 0.019 (± 9.1 %)
plain weave, glass fibre	923 ± 3 (± 0.3 %)	0.53 ± 0.00 (± 0.6 %)	95° ± 71°	1.240 ± 0.362 (± 29.2 %)	0.650 ± 0.167 (± 25.7 %)

Table 1. Examples for experimentally determined permeabilities: superficial density, S_0, fibre volume fraction, V_f, angle characterising orientation of principal permeability axes, θ, principal permeability values, K_1 and K_2; average values, standard deviations, and coefficients of variation (standard deviation/average) are given.

A dependence of the variability in the global permeability, characterised by the coefficient of variation, σ_K/K, on the scale of fabric non-uniformity, characterised by the in-plane yarn waviness, ω_{max}, relative to the specimen dimensions [2] is indicated qualitatively in Fig. 2.
These observations on global flow front propagation are complemented by three-dimensional mapping of the fluid concentration in reinforcement fabrics during impregnation (linear injection) applying Magnetic Resonance Imaging (MRI) techniques [3]. This allows meso-scale dry spots to be identified individually, and their development to be tracked, as shown in Fig. 3A for the example of a plain weave glass fibre fabric. Evaluation of the full 3D data set indicates that an observed dry spot does not move during impregnation, but changes shape and, due to the increasing local fluid pressure, decreases in size (from 155 mm^3 to 133 mm^3). The likely reason for dry spot formation is locally increased fibre volume fraction in the specimen, caused by non-uniformity of the yarn arrangement in each layer and effects of fabric nesting between layers.

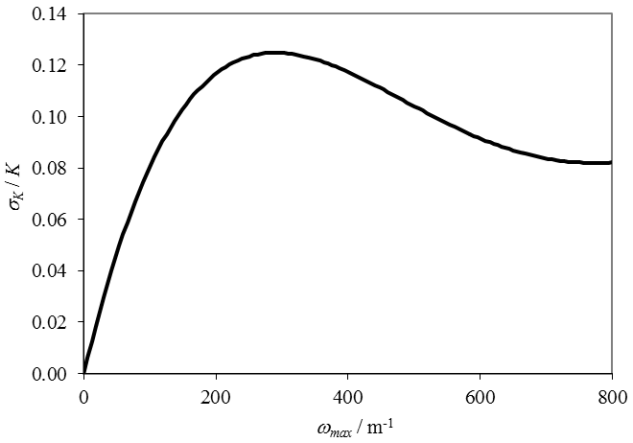

Figure 2. (Qualitative) dependence of coefficient of variation of global permeability, σ_K/K, measured in radial injection experiments for specimens of given dimensions, on the characteristic maximum frequency of yarn waviness, ω_{max}, describing the scale of fabric non-uniformity.

Monitoring of changes in local fluid concentration within fibre bundles, which reflects the micro-scale void content, indicates that, behind the flow front, a zone of partial saturation travels through the specimen. For each type of specimen, it has a characteristic width, which depends on the specimen properties and is related to the random arrangement of filaments within fibre bundles. Figure 3B indicates that for the example here, only warp yarns are impregnated in a zone of approximately 45 mm width between the flow front and the fully saturated part of the specimen.

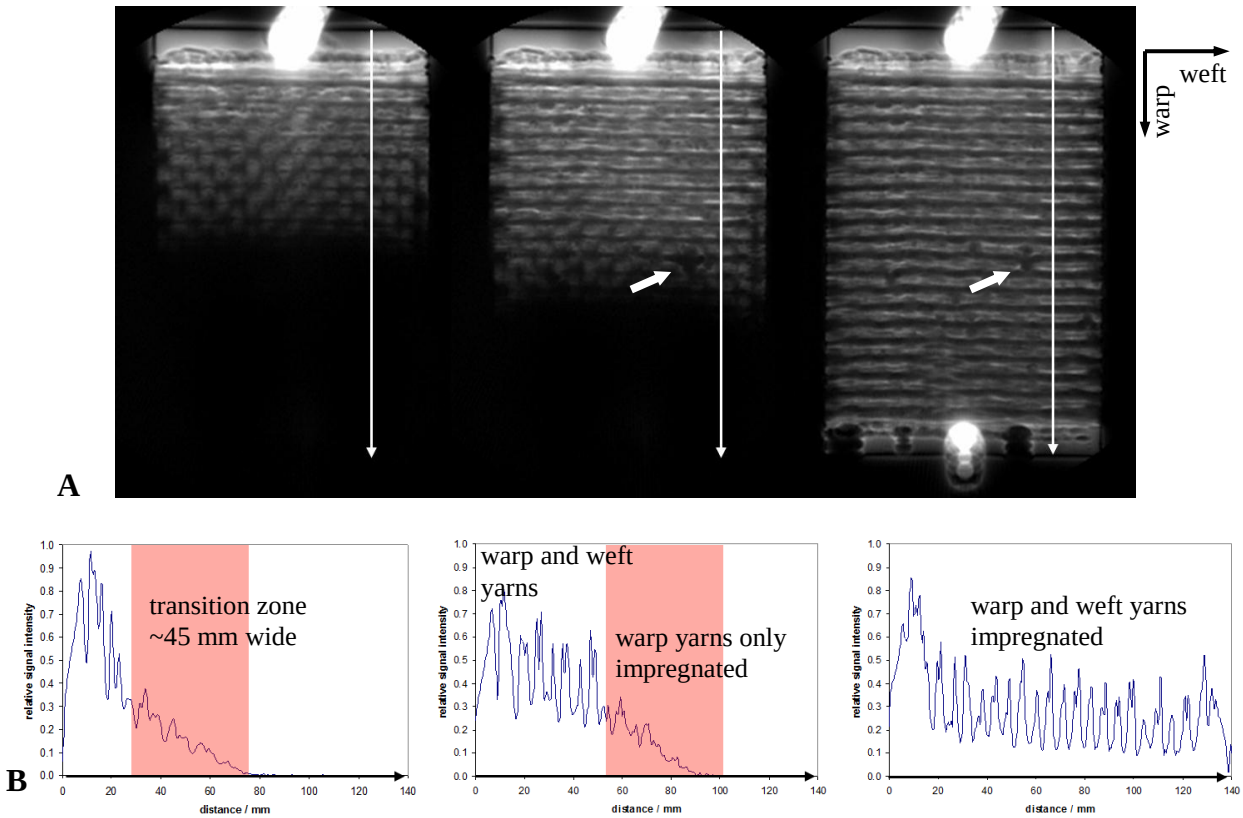

Figure 3. MRI scans showing the fluid concentration in plain weave E-glass fibre fabric at different levels of impregnation; A: slices from 3D data set; arrows indicate meso-scale dry spot; B: corresponding profiles of fluid concentration along indicated lines.

Micrographic analysis of composite specimens allows the typically non-uniform filament distribution within fibre bundles to be identified and micro-scale dry spots to be detected. For the example of a uni-directional carbon fibre fabric at different compaction levels, the filament arrangement was characterised by the typical distances between a filament and its *n*-th nearest neighbours (Fig. 4). The data suggest that, with increasing V_f, the average distance, *dn*, as a function of *n* converges to the step function for ideal (hexagonal) packing, implying that the filament distribution becomes more uniform with increasing level of bundle compaction.

The results of void content analysis (Table 2) allow the interpretation that, in transverse flow, there is a trend for the filament arrangement to become more uniform, and for the average void area (in cross-section), A_v, to decrease when the fibre bundle is compacted, i.e. when the specimen thickness, *h*, is reduced. This coincides with a reduced overall permeability, resulting in an increased number of voids, N_v, and therefore an increased overall void content. In longitudinal flow, the number of voids decreases significantly, while the typical void size increases with decreasing V_f, resulting in a decrease in total void content. This suggests that, at the given fibre volume fractions, dual-scale flow in between fibre bundles and within fibre bundles, which would favour a decrease in void content with increasing level of compaction due to more evenly distributed filaments, does not have a major effect on the yarn impregnation. At given V_f, the void content tends to be lower for longitudinal injection than for transverse injection, which is related to the generally higher average permeability.

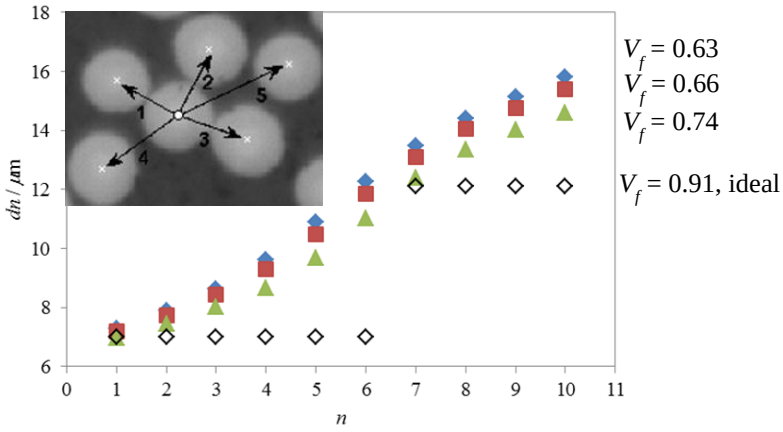

Figure 4. Distance between a filament and its *n*-th nearest neighbour, *dn*, at different fibre volume fractions, V_f, for the example of a uni-directional carbon fibre fabric.

	h / mm	V_f	N_v	A_v / 10^{-10} m^2	*void content*
transverse	0.32	0.55	16	21.48	2.3 %
	0.25	0.71	93	2.61	4.0 %
longitudinal	0.33	0.53	1	8.15	0.2 %
	0.25	0.71	34	2.72	1.6 %

Table 2. Void content in fibre bundles (sheets impregnated in uni-directional flow parallel or transverse to fibre bundle axis, 2 bar injection pressure); specimen thickness, *h*, global fibre volume fraction, V_f, number of voids per fibre bundle, N_v, average size of voids (characterised by area in cross-section), A_v, void content in terms of percentage of bundle cross-sectional area.

3 Numerical study

At the meso-/macro-scale, resin flow during impregnation of fibrous reinforcements was simulated applying Darcy's law to stochastic permeability fields. In a first approach, local permeability values were generated based on experimentally determined normal distributions of fibre angles in actual fabrics [4]. Typical results for flow front positions as a function of time for the example of an automotive component are plotted in Fig. 5. The distorted flow fronts in Fig. 5B look plausible qualitatively, but this approach is of limited use for simulating impregnation of fabrics, since it disregards the continuity of fibres.

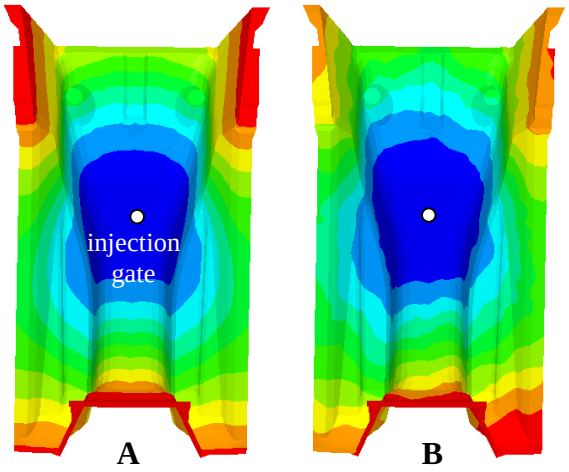

Figure 5. Flow front position as a function of time for an automotive component; A: ideal uniform reinforcement; B: hypothetical reinforcement with local fibre angles picked from experimentally determined distribution.

For fabrics from continuous fibre bundles, non-uniformity is described as in-plane yarn waviness. Characteristic random frequencies of waviness are related to experimentally observed fibre angle distributions in fabrics. Based on these frequencies, continuous permeability fields can be generated. Evaluating series of simulations with randomised parameters allows probable injection scenarios to be predicted. For geometrically simple cases as in Fig. 6, average value and standard deviation of the global permeability can be determined from the flow front positions at given injection times. For simulation of radial injections at realistic fibre volume fractions, coefficients of variation for the global permeability between 10 % and 20 % were determined, similar to the experimental results in Table 1. For geometrically more complex geometries, potential dry spots can be identified.

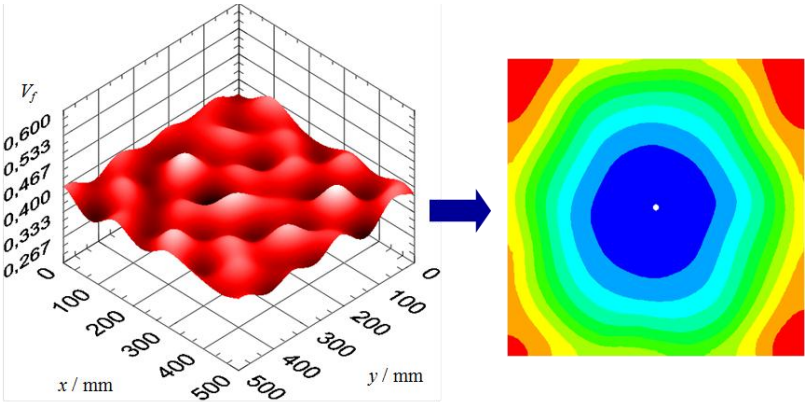

Figure 6. Non-uniform distribution of fibre volume fraction; corresponding flow front positions as a function of time for radial injection into a square flat plate.

For robot-produced chopped carbon fibre preforms for LCM processing of automotive components [5], geometrical preform models (Fig. 7A) are derived from properties of the chopped yarns and robot operating parameters. Permeability fields were approximated based on the local number of fibre bundles and their respective orientations. In the simulated flow front patterns (Fig. 7B), steep gradients of flow front positions at different injection times suggest high probability for void formation. Global permeability values derived from the simulations depend strongly on the modelling strategy for distribution of the chopped fibre bundles through the specimen thickness. The best agreement with experimentally determined permeability values was obtained when the fibre bundles were assumed to be evenly distributed through the preform thickness.

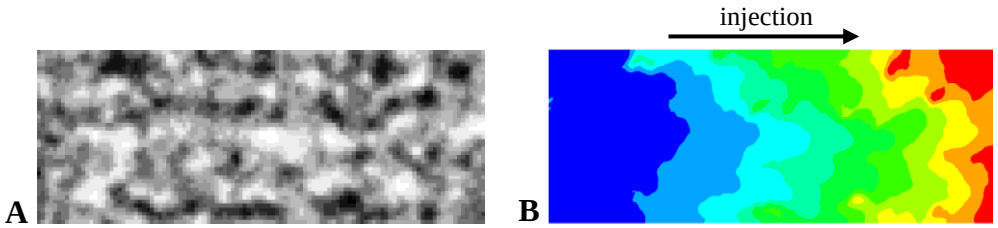

Figure 7. A: geometrical model; greyscales indicate local number of fibre bundles (dark: high; bright: low); B: simulated flow front patterns for linear resin injection at different injection times; steep gradients suggest high probability for void formation.

At the micro-scale, transverse flow through inter-filament gaps was analysed by Computational Fluid Dynamics simulation of Stokes flow. As flow domains, non-uniform filament arrangements, correlated to actual arrangements via the measured distances between neighbouring filaments (Fig. 4), were modelled in detail.
Results for the local flow velocity field in saturated flow (Fig. 8) indicate that most of the fluid is flowing through a few major flow channels which are formed in between clusters of filaments. Outside of these channels, the flow velocity is very low, suggesting that hardly any fluid will flow into the filament clusters. This implies that the probability for void formation in these zones is high. It is thought that, in histograms of the local flow velocities, increasing widths of distributions and the presence of peaks at low flow velocities are related to increased probability for void formation. While validation is still required, this would allow void content predictions to be made based on detailed analysis of flow velocity distributions obtained from steady state flow simulation.
Transverse permeabilities, derived from the applied pressure gradients and the calculated flow velocity fields, are log-normally distributed at any given fibre volume fraction. As the average permeabilities decrease with increasing fibre volume fraction, their scatter tends to decrease due to a reduction of the filament mobility. The permeabilities tend to be significantly smaller than the permeability calculated for ideal uniform filament arrangements (Fig. 9) according to Gebart [6]. This indicates the limitations of permeability predictions based on small periodic unit cells and the need to account for the statistical distribution of filaments within yarns.

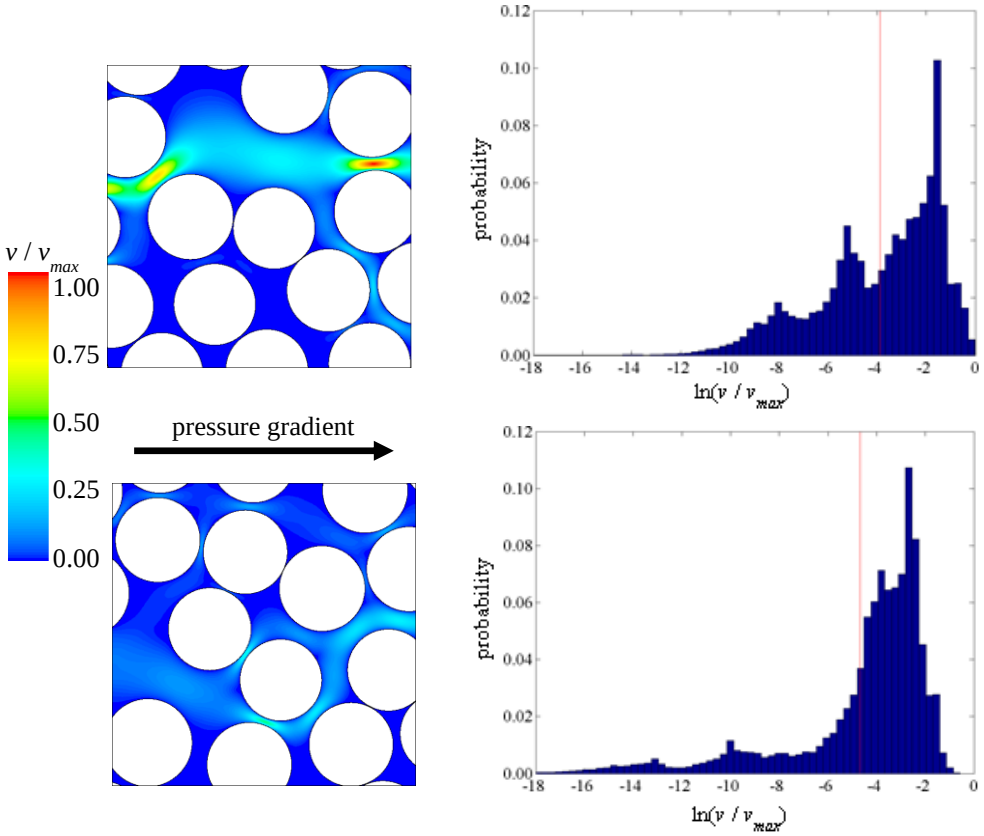

Figure 8. Maps of the magnitude of the flow velocity, v, normalised by the maximum observed velocity, v_{max}, for transverse flow through random filament arrangements, and histograms for the distributions of $\ln(v/v_{max})$.

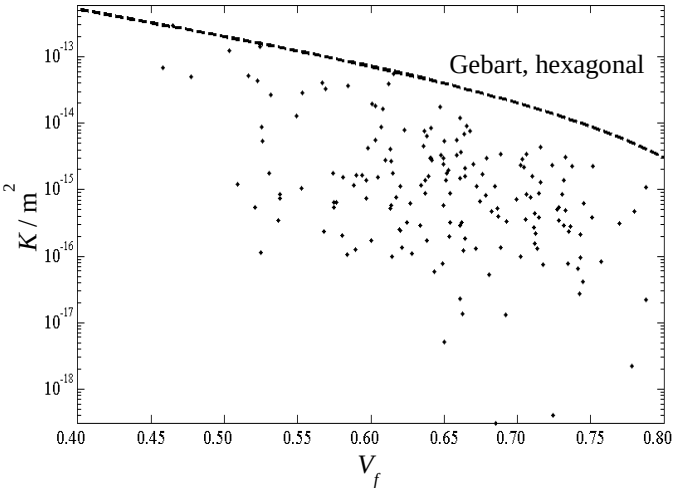

Figure 9. Numerical results for the transverse permeability, K, of a model with random filament arrangement as a function of the fibre volume fraction, V_f, compared to analytical solution based on Gebart's equations for a hexagonal filament arrangement.

4 Conclusions

The stochastic arrangements of yarns in fabrics and of filaments in yarns were characterised experimentally. At the macro-scale, the influence of non-uniform distributions of yarns on impregnating resin flow was quantified in terms of global permeability values and their variability. At the meso- and micro-scale, local fluid distributions were mapped and dry spot development during fabric impregnation was tracked.

Geometrical models were developed for non-uniform yarn distributions in fabrics and random preforms from chopped fibres. These allow realistic mould filling patterns to be simulated and the variability in global permeability to be estimated. Modelling non-uniform filament distributions in yarns allows yarn permeabilities to be derived, which differ significantly from ideal values, and potential dry spot formation to be detected.
The work described here will be continued within the framework of the newly established EPSRC Centre for Innovative Manufacturing in Composites with particular focus on

- meso-scale flow and cure simulation to predict manufacturing defects arising from material and process variability,
- macro-scale transient flow simulation for a reactive resin system allowing the range of possible outcomes to be predicted at component scale,
- structural finite element analysis for samples and components incorporating defects to predict their effects mechanical behaviour,
- experimental validation of predicted defects at all scales and their effects on mechanical performance using mechanical testing and state-of-the-art imaging techniques.

Acknowlegements
This work was funded by the Engineering and Physical Science Research Council as part of Platform Grant, EP/F02911X/1, and the Nottingham Innovative Manufacturing Research Centre, EP/E001904/1.

References

[1] Endruweit A., Ermanni P. The In-Plane Permeability of Sheared Textiles. Experimental Observations and a Predictive Conversion Model. *Compos Part A-Appl S*, **35**, pp. 439-451 (2004).
[2] Endruweit A., McGregor P., Long A.C., Johnson M.S. Influence of the fabric architecture on the variations in experimentally determined in-plane permeability values. *Compos Sci Technol*, **66**, pp. 1778-1792 (2006).
[3] Endruweit A., Glover P., Head K., Long A.C. Mapping of the fluid distribution in impregnated reinforcement textiles using Magnetic Resonance Imaging: Application and discussion. *Compos Part A-Appl S*, **42**, pp. 1369-1379 (2011).
[4] Endruweit A., Long A.C., Robitaille F., Rudd C.D. Influence of stochastic fibre angle variations on the permeability of bi-directional textile fabrics. *Compos Part A-Appl S*, **37**, pp. 122-132 (2006).
[5] Endruweit A., Harper L.T., Turner T.A., Warrior N.A., Long A.C. Random discontinuous carbon fibre preforms: Permeability modelling and resin injection simulation. *Compos Part A-Appl S*, **39**, pp. 1660-1669 (2008).
[6] Gebart B.R. Permeability of Unidirectional Reinforcements for RTM. *J Compos Mater*, **26**, pp. 1100-1133 (1992).